Calibration Study of a Continuously Variable Transmission System Designed for pHRI

Emir Mobedi[1], Mehmet İsmet Can Dede[2]

[1]*Italian Institute of Technology, Italy, e-mail: emir.mobedi@iit.it*

[2]*Izmir Institute of Technology, Turkey, e-mail: candede@iyte.edu.tr*

Abstract.

Variable stiffness actuators (VSAs) have been used in many applications of physical human-robot interfaces (pHRI). A commonly employed design is the spring-based VSA allowing the user to regulate the output force mechanically. The main design criteria of these actuation systems are the adjustment of output force independent from the output motion, and shock absorbing. In our recent work, we implemented certain modifications on the two-cone friction drive continuously variable transmission system (CVT) so that the CVT can be employed in pHRI systems. Subsequently, the optimized prototype is developed. In this study, we introduce the prototype of this new CVT systems, and its force calibration tests. The results indicate that the manufactured CVT is capable of displaying the desired output force throughout its transmission ratio range within a tolerance.

Key words: Continuously variable transmission (CVT), Variable stiffness actuation (VSA), physical Human-robot interface

1 Introduction

In early industrial robot applications, robots were operating in a working cell isolated from the working area of the human co-workers due to the safety reasons. Following the establishment of ISO 10218-1 standards, collaborative robots emerged in the industrial settings [1]. These robots are capable of regulating their physical interaction by the employment of compliant control methods [2] and/or with the help of specific mechanical solutions [3]. The latter one, which is most commonly developed and termed as VSAs, requires certain design requirements such as independent torque and motion variation [4]. In our recent work, we proposed a new CVT design by considering the aforementioned criteria [5]. In the design phase, the fundamental modification is carried out by changing the transmission wheel with a sphere allowing the transmission variation independent from output motion. However, as a result of this solution, new problems arise related to the bidirectional transmission adjustment. In the clock-wise (CW) direction, the

transmission can be achieved without any slip within the nominal torque transmission limits since the tangential friction forces pull the sphere into the cones (Figure 1.a). However, in the counter-clock-wise (CCW) direction, tangential friction forces push the sphere out of the cones, and this leads to slippage at the contact points even though the nominal transmission torque is not violated (cone-sphere, Fig 1.b). To overcome this problem, a second sphere, which is drawn with a red dashed circle in Figure 1.b, is added to the system. Additionally, spring with pretension are used to push the spheres to the cones to form an equal amount of normal force at the friction surfaces (F_1 and F_2 in Figure 1.b). The isometric view of the system is illustrated in Figure 1.c.

In this paper, the work carried out for the force calibration of this new CVT is presented. The next section presents the test setup for the calibration procedure.

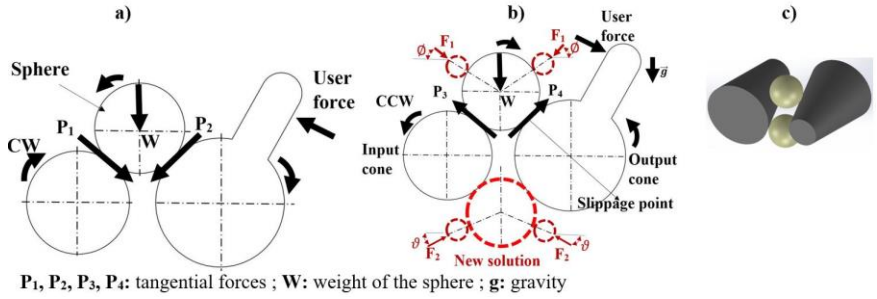

Fig 1. The illustration of the new CVT: (a) The working principle of the single-sphere CVT, (b) The double-sphere CVT, (c) Isometric view of the double-sphere CVT

2 The test setup of the new CVT system

In this section, test setup for the calibration procedure of the new CVT is introduced, which is presented in Figure 2. The CVT system is composed of the two cones, a carriage with two spheres, an input torque motor (Motor-1), and a linear motion system coupled to a motor (Motor-2) that changes the location of the transmission elements (the spheres) which is shown in Figure 2.b.

In the test setup, the following components are used; (1) a force sensor (Kistler, type 9017B) that is fixed to the handle to measure the output force, (2) a capstan drive to transmit the output cone's torque to the handle, (3) three absolute encoders (MagAlpha, TBMA702-Q-RD-00A) to observe whether there are slippages between the cones and the spheres, and the capstan drive. The encoder that appears on the right side of Figure 2.a is coupled to Motor-2 so that a closed-loop position control is employed to move the carriage mechanism that is changing the location of the spheres (Z distance).

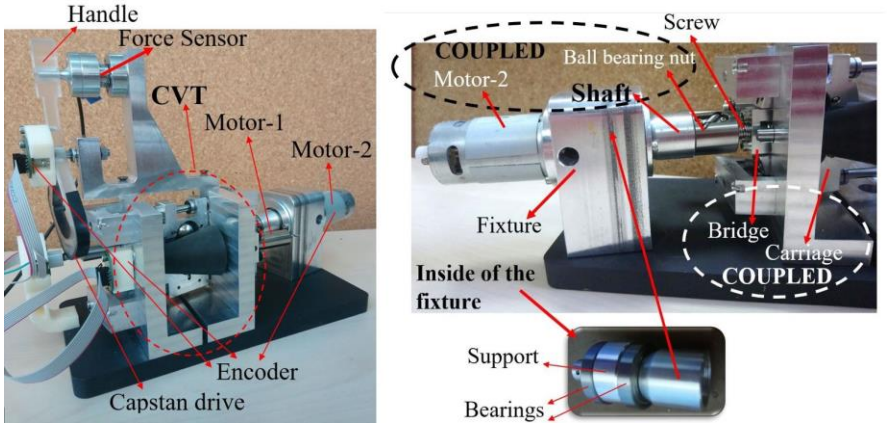

(a) (b)

Fig 2. Illustrations of the new CVT: (a) The CVT prototype (b) The design of the linear motion mechanism

The friction material covering the cones is chosen as EPDM rubber with 70 shore hardness. The neoprene material used in HAPKIT [6] is the basis for this selection, which has also the same shore value. After the cones are covered with the friction material, cones' angle (θ), length (L), and the minimum cone radii (r_1) are measured by a profile projector machine (Mitutoyo) (a contactless measurement method). The measurement results are presented in Table 1.

Table 1. Comparison between the desired and the measured dimensions of the

# of the cone	r_1 (mm)	θ (rad)	L (mm)
1	9.4635	12.2883°	49.57
2	9.4525	12.3122°	50.08
Selected values	**9.455**	**12.295°**	**49.825**
Desired values	9	12.5°	50.76

The difference the measured and designed parameters is the manufacturing errors due to the manufacturing process with grinding, CNC milling, and turning machines. Therefore, the tests are conducted by using the average of the measured dimensions of the cones, which are stated as the selected values in Table 1.

3 The output force calibration of the CVT

The aim of this experiment is to observe if the desired maximum output force can be reached, which is selected as 6 N by considering the HAPKIT limitations [6]. The handle's dimensions are illustrated in Figure 3.

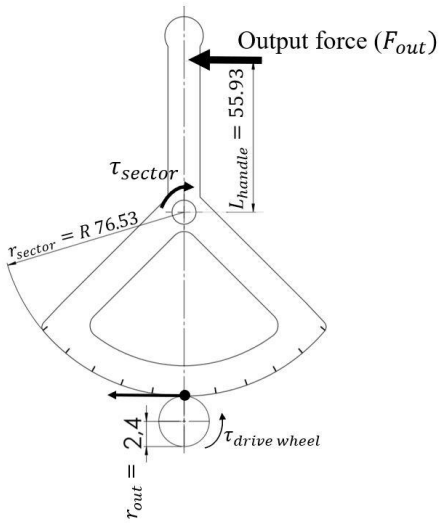

Fig 3. The illustration of the dimensions of the HAPKIT v2.0

Accordingly, output torque of the CVT system, $\tau_{drivewheel}$, is calculated with respect to the presented dimensions in the following equations.

$$\tau_{sector} = F_{out}L_{handle} = (6)(55.93) = 335.58 \text{ mNm} \quad (1)$$

$$\tau_{drive\ wheel} = \tau_{sector}\frac{r_{out}}{r_{sector}} = (335.58)\frac{(2.40)}{(76.53)} = 10.523 \text{ mNm} \quad (2)$$

Finally, the input torque to be supplied to the input cone is calculated (τ_{in}) is presented in Equation (3).

$$\tau_{in} = \frac{\tau_{drivewheel}r_2}{r_3\delta} \quad (3)$$

In Equation (3), r_2 and r_3 represents the effective input and output cone radii, respectively. The derivation of these parameters is carried out in [5]. δ is varying between 0.97 and 0.99, which is a function of the spheres' location (Z). This δ parameter is obtained as a result of force analyses, which is not presented in this paper due to space considerations. To calculate the necessary current, the torque constant of the Motor-1 (7.3 $mNmA^{-1}$) is considered.

At the beginning of the experiment, the tests are conducted by taking into account the calculated input torque values (theoretical torques) according to Equation 3. First, the carriage mechanism is located at the initial position where the transmission ratio is at the minimum level ($Z = 46.5461$ mm).

When lower input torques are applied to the input cone, the output force is not changed, hence, the transmission is not achieved between the cones. The reason for this problem is the manufacturing errors and the viscoelastic behavior of the friction material. During the bias torque experiments, observation of a minimum of 0.05 N force change at the handle is required to set the torque value as the bias torque.

In Figure 4, the data set, including measured force, applied current, and the positions of the handle, output cone, and input cone is presented for the location of the spheres at $Z = 36.54$ mm. According to this Figure, the measured output force reaches the peak point at 0.6 seconds, and then slightly decreases. The issue stems from the viscoelastic behavior of the friction material, which is commonly known as the relaxation of the rubber. Therefore, the measured force values are recorded after the relaxation period. For instance, in Figure 5, the recorded force values are between 1-1.2 seconds. On the other hand, the angular position of the input cone changes during this interval since the spheres are pressed inside the cones when the input torque is supplied to the system. In the course of this period, the angular positions of the cones are changed, and after the torque transmission is stopped, they are move back with a slight error with respect to their original positions. Nevertheless, this situation prevents both the actuator and the user from unexpected impacts, which is defined in the literature as shock absorbing phenomenon for VSAs [3].

During the force calibration experiments, maximum 5° slippage between the cones is taken as an acceptable position error.

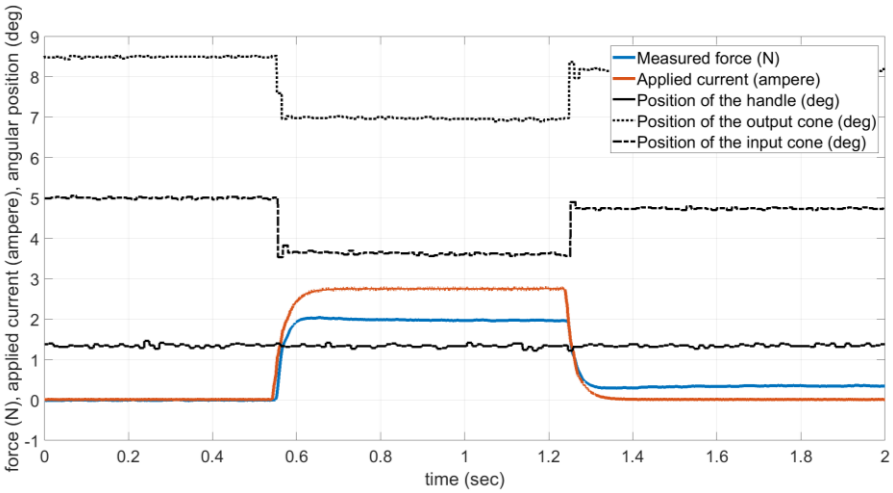

Fig 4. The data set illustration for $Z = 36.54$ mm

The results of the non-calibrated experiment are presented in Figure 5. The red dashed lines at ±6 N presents the desired output forces at each direction. At each test point, the experiment is conducted for three times to check whether the repeatable data is acquired.

Moreover, it is clear that, as the carriage mechanism with the spheres approaches to the point where the output cone diameter is at its maximum value, the measured output force reaches the minimum level. In other words, even if it is expected to obtain the same output force value (6 N) in all the test points, the efficiency of the CVT reduces as the ratio between the input and output cone contact radii decreases. This situation is defined in the literature as the spin effect leading to extra rotation on the sphere [7].

Another phenomenon that is experienced in the tests is when the torque is applied to the input cone, the viscoelastic material covered on the cones is compressed by the sphere. It is as if a spring is compressed. After a test, if a second experiment is conducted, the measured force is decreased since the spheres submerged into the cones. Hence, after each experiment, an inverse torque is applied to the CVT so that there is no energy accumulation within the friction material. The value of the release term is selected as 0.5 A.

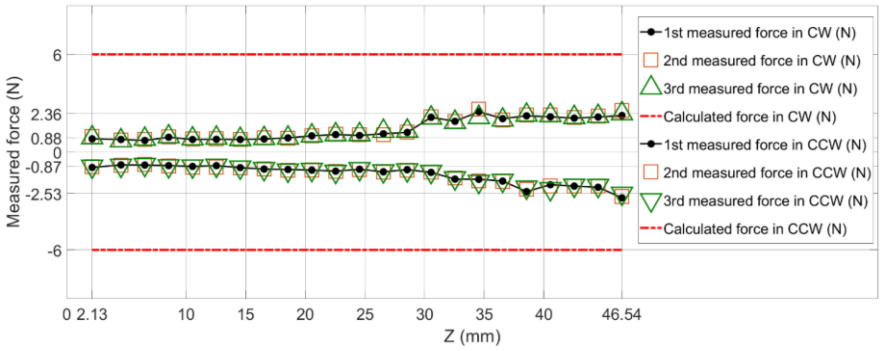

Fig 5. The results of the non-calibrated desired continuous output force experiment

In the calibration experiment set, the current of the motor-1 is regulated manually to result in the desired output force, which is 6N, at the handle. Moreover, the release term is set precisely for each test point to acquire repeatable force data.

In Figure 6, the calibration results are illustrated. Consequently, it is observed that the CVT system is capable of displaying the desired force with repeatable data. The tolerance is chosen as 6 ± 0.3 N. In the same fashion of the non-calibrated experiment, at each test point, the experiment is conducted three times in each direction.

Also, considering the applied current, there is a similar trend for both CW and CCW directions. This means that the pretension of the spring forces is close to each other for the upper and lower sphere, and the covering of the cones with the friction material is achieved with minimal errors. The reason why the applied currents for

CW direction is greater than CCW is that the normal force of the upper sphere cannot be adjusted precisely because of the gravitational load. On the other hand, the normal force of the lower sphere can be regulated as the pretension springs compensate both its gravity and the normal force from the lower part.

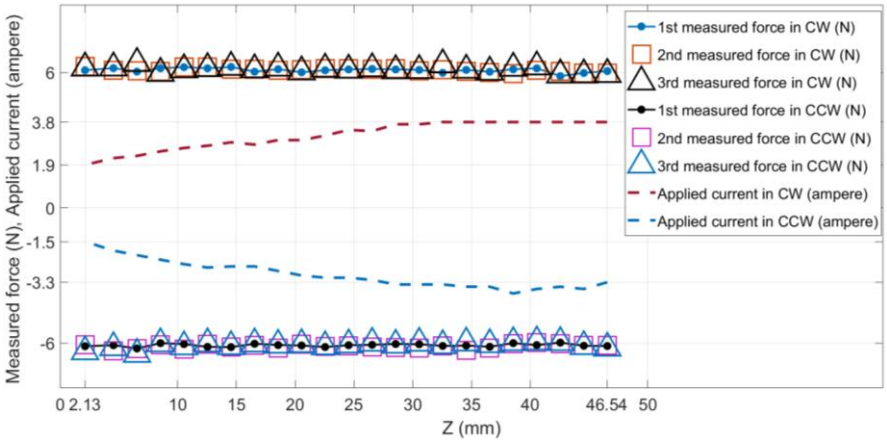

Fig 6. The results of the calibrated desired continuous output force experiment

5 Conclusions

In this study, the force calibration of a recently developed CVT mechanism is presented. Results show that the proposed CVT has the capability to display 6 N output force which was assigned by considering the HAPKIT output force capabilities [6]. As a future study, we will introduce the optimization methodology of this new CVT based on its static force and spin effect analyses.

Acknowledgments This work is supported in part by The Scientific and Technological Research Council of Turkey via grant number 117M405.

References

1. Peternel, L., Tsagarakis, N., and Ajoudani, A. : A Human-Robot Co-Manipulation Approach Based on Human Sensorimotor Information. IEEE Transactions on Neural Systems and Rehabilitation Engineering, 25, 811-822 (2017).
2. Salisbury, J.K.: Active Stiffness Control of a Manipulator in Cartesian Coordinates. IEEE Conference on Decision and Control including the Symposium on Adaptive Processes, 95-100 (1980).
3. Wolf, S., and Hirzinger, G.: A New Variable Stiffness Design: Matching Requirements of the Next Robot Generation. IEEE International Conference on Robotics and Automation, 1741-46 (2008).

4. Tonietti, G., Schiavi, R., and Bicchi, A.: Design and Control of a Variable Stiffness Actuator for Safe and Physical Human-Robot Interaction. IEEE International Conference on Robotics and Automation, 526-31 (2005).
5. Mobedi, E., and Dede, M.İ.C.: Geometrical Analysis of a Continuously Variable Transmission System Designed for Human-Robot Interfaces, Mechanism and Machine Theory, 140, 567-85 (2019).
6. Martinez, M. O., Morimoto, T. K., Taylor, A. T., Barron, A. C., Pultorak, J. D. A., Wang, J., Kaiser, A. G., Davis, R. L., Blikstein, P., and Okamura, A. M.: 3-D Printed Haptic Devices for Educational Applications. In Proceedings of the IEEE Haptics Symposium, 126–133 (2016).
7. De Novellis, L., Carbone, G., and Mangialardi L. Traction and Efficiency Performance of the Double Roller Full-Toroidal Variator: A Comparison With Half- and Full-Toroidal Drives, Journal of Mechanical Design, Vol.134, No.7, pp. 1-14 (2012).